

Role of Three-Nucleon Forces in Neutron-Rich Nuclei Beyond ^{132}Sn

L. CORAGGIO¹, A. GARGANO¹, and N. ITACO^{1,2}

¹*INFN, Complesso Universitario di Monte S. Angelo, via Cintia, 80126 Napoli, Italy*

²*Dipartimento di Fisica, Università di Napoli “Federico II”, Complesso Universitario di Monte S. Angelo, via Cintia, 80126 Napoli, Italy*

E-mail: coraggio@na.infn.it

(Received September 11, 2014)

The role of three-nucleon forces (3NF) in the description of nuclear structure properties is nowadays a main topic in the field of microscopic many-nucleon calculations. We investigate the relative weight between effective two- and three-nucleon forces in neutron-rich nuclei beyond the doubly-closed ^{132}Sn core within the realistic shell-model framework, studying the evolution of the spectroscopic properties of $N = 82$ isotones and heavy tin isotopes. This problem is tackled indirectly without explicitly taking into account effective 3NF through the comparison of the results of shell-model calculations obtained from realistic on-shell-equivalent low-momentum potentials.

KEYWORDS: Nuclear shell model, realistic nucleon-nucleon potentials, effective interactions

1. Introduction

The study of the effects of 3NF is currently a relevant issue in nuclear structure calculations for many-body systems [1–4]. The renormalization of a high-momentum realistic high-precision nucleon-nucleon (NN) potential via the $V_{\text{low-k}}$ [5, 6] or the similarity-renormalization group (SRG) [7] approaches provides on-shell-equivalent NN interactions which are suitable for perturbative many-body calculations, and that are characterized by a cutoff parameter Λ . Actually, starting from these on-shell equivalent NN potentials the results of calculations for few-body and infinite systems are dependent from the chosen cutoff owing to their different off-shell behavior, and the cutoff independence can be restored introducing many-body forces aside the NN one [8, 9].

As a matter of fact, in the effective field theory (EFT) framework - where both $V_{\text{low-k}}$ and SRG approaches are grounded - the calculated physical observables are ideally independent of the cutoff scale Λ , provided that nuclear two- and many-body forces are taken into account [10]. For nuclear potentials this can be done by way of the chiral perturbation theory (ChPT), which introduces nuclear two-, three-, four-, ... body interactions on an equal footing [11, 12] able to reproduce accurately the nucleon-nucleon (NN) data [13].

The regulator dependence of chiral potentials in many-body systems has been recently investigated in both neutron and nuclear infinite matter [14, 15], where the NNN potential has been explicitly taken into account. In particular, in [14] it has been evidenced the crucial role of the NNN potential in order to provide the cutoff independence in infinite neutron matter.

The computational problem of including a 3NF in finite-nuclei calculations is far more complicated than in infinite nuclear systems, so in present paper we have faced this problem indirectly without explicitly taking into account these forces.

We have studied the relative weight between effective two- and three-nucleon forces in neutron-rich nuclei beyond the doubly-closed ^{132}Sn core within the realistic shell-model framework.

To this end, starting from the high-precision NN potential CD-Bonn [16], we have derived two

on-shell-equivalent low-momentum potentials by way of the $V_{\text{low-k}}$ approach [6]. These two potentials, which reproduce exactly the same two-nucleon-system data of the original CD-Bonn potential, differ because they are defined up to two cutoffs $\Lambda = 2.1$ and 2.6 fm^{-1} .

As mentioned before, these potentials do not yield identical results in the many-body problems, as testified by the different values of the triton and ^4He binding energies, and the differences should be eliminated taking into account the 3NF corresponding to the chosen cutoff and derived so as to reproduce the original-potential value of the triton binding energy [8, 9].

Starting from these two $V_{\text{low-k}}$ s, we have derived the effective shell-model hamiltonians within the framework of the time-dependent degenerate linked-diagram perturbation theory [17]. This approach provides both the single-particle (SP) energies and the two-body matrix elements (TBME) of the residual potential without resorting to any parameter fitted to experimental data [18].

We have performed then shell-model calculations for nuclei outside the doubly-closed ^{132}Sn , focusing our attention on the evolution of the spectroscopic properties of the $N = 82$ isotones and heavy-mass tin isotopes when adding valence nucleons. This region is currently the subject of great experimental and theoretical interest, especially in view of the production of new neutron-rich nuclear species at the next generation of radioactive ion beam facilities, in order to study the shell evolution versus the number of the valence nucleons.

In the following section, we outline the perturbative approach to the derivation of a realistic shell-model hamiltonian. In Section 3, we present the results of our shell-model calculations, performed by using the Oslo shell-model code [20], and compare them with the experimental data to infer the role of the missing 3NFs. A short summary is given in the last section.

2. Outline of calculations

As mentioned in the Introduction, we derive the shell-model effective hamiltonians within the framework of the time-dependent degenerate linked-diagram expansion [19].

To this end, an auxiliary one-body potential U is introduced to write down the hamiltonian as the sum of an unperturbed term H_0 , which describes the independent motion of the nucleons, and a residual interaction H_1 :

$$H = \sum_{i=1}^A \frac{p_i^2}{2m} + \sum_{i < j} V_{NN}^{ij} = T + V_{NN} = (T + U) + (V_{NN} - U) = H_0 + H_1 \quad ,$$

where V_{NN} represents the input NN potential.

The effective hamiltonian H_{eff} is obtained by way of the Kuo-Lee-Ratcliff folded-diagram expansion in terms of the vertex function \hat{Q} -box, which in the perturbative approach is built by a collection of irreducible valence-linked diagrams [17]. We calculate the \hat{Q} -box including one- and two-body Goldstone diagrams through third order in H_1 [18]. Calculations beyond the third order in perturbation theory are computationally prohibitive, so we have calculated the Padé approximant [21] [21] of the \hat{Q} -box to obtain a value to which the perturbation series should converge, as suggested in [22]. The folded-diagram series is then summed up to all orders using the Lee-Suzuki iteration method [23].

The \hat{Q} -box contains one-body contributions, whose collection is the so-called \hat{S} -box [24]. The folded-diagram expansion of the \hat{S} -box represents the theoretical SP energies, that will be employed in the shell-model calculations. The TBME will be then obtained by way of a subtraction procedure of these SP energies from H_{eff} .

As mentioned in the Introduction, we employ as V_{NN} a low-momentum potential $V_{\text{low-k}}$ defined within a cutoff momentum Λ by way of a similarity transformation [6]. This is a smooth potential which preserves exactly the on-shell properties of the original V_{NN} and is suitable for being used directly in nuclear structure calculations [19].

We have derived from the high-precision CD-Bonn NN potential [16] two $V_{\text{low-k}}$ s corresponding

to $\Lambda = 2.1$ and 2.6 fm^{-1} .

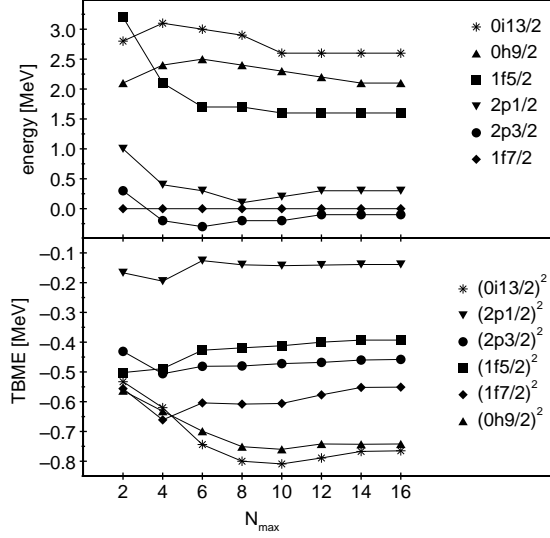


Fig. 1. Theoretical single-neutron relative energies (up) and neutron-neutron diagonal $J^\pi = 0^+$ TBME (down) as a function of N_{\max} (see text for details).

It is worth to spend a few lines about the convergence properties of the theoretical SP energy spectra and TBME as a function of the dimension of the intermediate-state space. In Fig. 1, we report the single-neutron relative energy spectrum and the diagonal $J^\pi = 0^+$ TBME of the tin isotopes calculated with the cutoff $\Lambda = 2.6 \text{ fm}^{-1}$ as a function of the maximum allowed excitation energy of the intermediate states expressed in terms of the oscillator quanta N_{\max} . We show results with $\Lambda = 2.6 \text{ fm}^{-1}$ because the larger is the cutoff the slower is the convergence rate. From Fig. 1 it is clear that our results have practically achieved convergence at $N_{\max} = 16$.

3. Results and comparison with experiment

In Fig. 2 the theoretical SP spectra of ^{133}Sb and ^{133}Sn are compared with the experimental ones [25]. They are normalized with respect to the proton $0d_{5/2}$ state and neutron $1f_{7/2}$, respectively, in order to evidence the changes in the spacings with the cutoff Λ . It has to be pointed out that there is no experimental counterpart for the proton $2s_{1/2}$ orbital and that the neutron $0i_{13/2}$ energy in [25] is estimated as in [26] from the observed 10^+ state at 2434 keV in ^{134}Sb .

From the inspection of Fig. 2, it can be seen that the calculated spin-orbit splitting between $1d_{3/2}$ and $1d_{5/2}$ levels is scarcely dependent on Λ , the experimental separation being reasonably well reproduced.

The situation is quite different for the calculated relative energies of the $0g_{7/2}$ and $0h_{11/2}$ levels, whose spin-orbit partners are outside the chosen model space. In this case, the theoretical values show a strong dependence on the cutoff Λ . The most striking feature is that for $\Lambda = 2.1 \text{ fm}^{-1}$ the discrepancies with respect to the experimental data are quite large, while a better agreement is obtained with $\Lambda = 2.6 \text{ fm}^{-1}$. In particular, it should be pointed out that with $\Lambda = 2.1 \text{ fm}^{-1}$ the $0h_{11/2}$ level lies far away from the other levels, thus implying an enhanced shell closure at $Z = 70$. A much more reasonable spectrum of ^{133}Sb is obtained when using $\Lambda = 2.6 \text{ fm}^{-1}$ with the intruder $0h_{11/2}$ proton state joining the 50-82 shell.

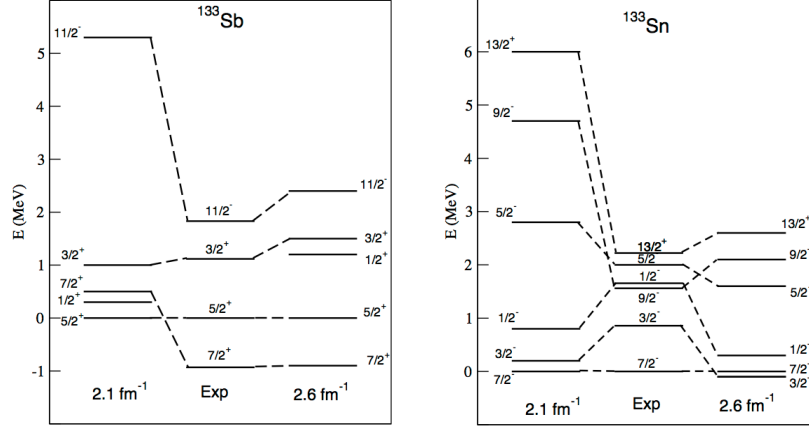


Fig. 2. Calculated and experimental single-particle spectra of ^{133}Sb and ^{133}Sn . The spectra are normalized with respect to $J = 5/2^+$ and $J = 7/2^-$ levels, respectively.

The inspection of Fig. 2 shows that similar conclusions can be drawn for the single-neutron energies. In fact, the $0h_{9/2}$, $0i_{3/2}$ relative energies are quite sensitive to the choice of the cutoff, and a better agreement with experiment is obtained with $\Lambda = 2.6 \text{ fm}^{-1}$.

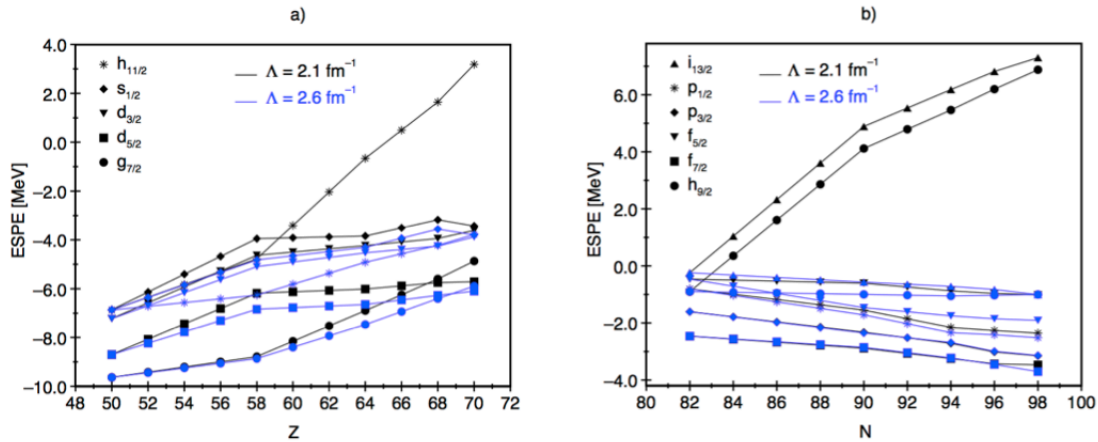


Fig. 3. Calculated effective single-particle energies for the $N = 82$ isotones (a) and heavy tin isotopes (b). The continuous black line refers to calculations performed with $\Lambda = 2.1 \text{ fm}^{-1}$, the blue one to $\Lambda = 2.6 \text{ fm}^{-1}$.

The sensitivity to the cutoff value shown by the SP relative energies of the orbitals with the spin-orbit partner outside the model space is found also in the monopole component of the TBME. In Fig. 3 we report the proton and neutron effective single-particle energies (ESPE) calculated with both $\Lambda = 2.1$ and 2.6 fm^{-1} as a function of Z and N , respectively. We have employed the experimental

SP energies available from the ^{133}Sb and ^{133}Sn data [25], in order to evidence the role of the cutoff on the monopole term. As for the proton $2s_{1/2}$ orbital, the SP energy has been taken as the empirical value in [19].

It can be seen that the $\pi 0h_{11/2}$, $\nu 0h_{9/2}$, and $\nu 0i_{13/2}$ ESPE exhibit a strong repulsive behavior when employing $\Lambda = 2.1 \text{ fm}^{-1}$, while for the $\pi 0g_{7/2}$ ESPE this is far less marked. In particular, according to $\Lambda = 2.1 \text{ fm}^{-1}$ calculations it should appear a strong shell closure at $Z = 70$ and at $N = 102$.

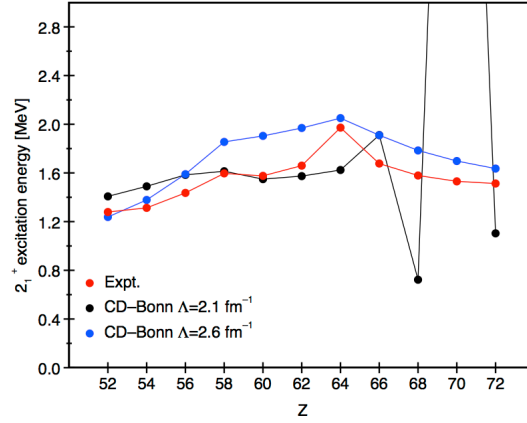


Fig. 4. Calculated and experimental excitations energies of the yrast $J = 2^+$ states for the $N = 82$ isotones. The continuous black line refers to calculations performed with $\Lambda = 2.1 \text{ fm}^{-1}$, the blue one to $\Lambda = 2.6 \text{ fm}^{-1}$.

In Fig. 4 the behavior of the calculated and experimental excitation energies of the yrast $J = 2^+$ states for the $N = 82$ isotones is reported. Experimental data evidence a subshell closure at $Z = 64$ for ^{146}Gd and no shell closure at $Z = 70$ for ^{152}Yb , correctly reproduced with the cutoff $\Lambda = 2.6 \text{ fm}^{-1}$. On the other side $\Lambda = 2.1 \text{ fm}^{-1}$ results loose any meaning from $Z = 64$ since they do not take into account the role played by the $\pi 0h_{11/2}$ orbital. For the sake of completeness, in Fig. 5 we report the behavior of the excitation energies of the yrast $J = 2^+$ states for the heavy tin isotopes, but the calculations could not be carried out beyond $N = 90$ owing to the computational complexity.

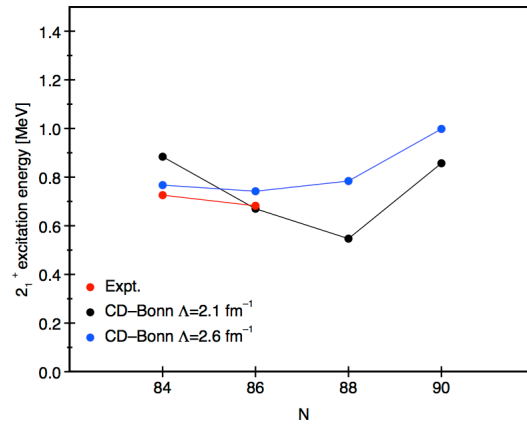


Fig. 5. Same as in Fig. 4, but for the heavy tin isotopes.

To summarize, the results of our calculations show that both SP energies and monopole properties of the orbitals without their own spin-orbit partner in the chosen model space are quite sensitive to the cutoff value. We can then infer that these quantities are sensitive to the missing 3NF too. Finally, the comparison with the available data shows that, since the inclusion of the 3NF should eliminate - or at least reduce - the cutoff dependence and provide a better agreement with experiment, the larger the cutoff the smaller is the role of the missing 3NF.

4. Summary

In this paper we have presented the results of a study of the role of 3NF in realistic shell-model calculations for nuclei beyond doubly-closed ^{132}Sn . In particular, we have focused our attention on the $N = 82$ isotonic and the heavy tin isotopic chains, employing effective shell-model hamiltonians derived from two low-momentum on-shell-equivalent potentials characterized by two different cutoffs.

Our investigation of the 3NF relevance has been carried out indirectly, by comparing the results with the cutoffs $\Lambda = 2.1$ and 2.6 fm^{-1} and tracing back the sensitivity to this parameter to the role of the missing 3NF.

The results show that the orbitals lacking their spin-orbit partner in the chosen model space are quite affected by the cutoff value, a better agreement with experiment being obtained when employing a larger cutoff.

References

- [1] P. Navrátil, V. G. Gueorguiev, J. P. Vary, W. E. Ormand, and A. Nogga: Phys. Rev. Lett. **99** (2007) 042501.
- [2] G. Hagen, T. Papenbrock, D. J. Dean, A. Schwenk, A. Nogga, M. Włoch, and P. Piecuch: Phys. Rev. C **76** (2007) 034302.
- [3] G. Hagen, M. Hjorth-Jensen, G. R. Jansen, R. Machleidt, and T. Papenbrock: Phys. Rev. Lett. **109** (2012) 032502.
- [4] V. Somà, A. Cipollone, C. Barbieri, P. Navrátil, and T. Duguet: Phys. Rev. C **89**, (2014) 061301(R).
- [5] S. Bogner, T. T. S. Kuo, L. Coraggio: Nucl. Phys. A **684** (2001) 432.
- [6] S. Bogner, T. T. S. Kuo, L. Coraggio, A. Covello, and N. Itaco: Phys. Rev. C **65** (2002) 051301(R).
- [7] S. K. Bogner, R. J. Furnstahl, and A. Schwenk : Prog. Part. Nucl. Phys. **65** (2010) 94.
- [8] A. Nogga, S. K. Bogner, and A. Schwenk: Phys. Rev. C **70** (2004) 061002(R).
- [9] S. K. Bogner, A. Schwenk, R. J. Furnstahl, and A. Nogga: Nucl. Phys. A **763** (2005) 59.
- [10] U. van Kolck: Prog. Part. Nucl. Phys. **43** (1999) 337.
- [11] S. Weinberg: Phys. Lett. B **295** (1992) 114.
- [12] U. van Kolck: Phys. Rev. C **49** (1994) 2932.
- [13] R. Machleidt and D. R. Entem: Phys. Rep. **503** (2011) 1.
- [14] L. Coraggio, J. W. Holt, N. Itaco, R. Machleidt, and F. Sammarruca: Phys. Rev. C **87** (2013) 014322.
- [15] L. Coraggio, J. W. Holt, N. Itaco, R. Machleidt, L. E. Marcucci, and F. Sammarruca: Phys. Rev. C **89** (2014) 044321.
- [16] R. Machleidt: Phys. Rev. C **63** (2001) 024001.
- [17] T. T. S. Kuo, S. Y. Lee, and K. F. Ratcliff: Nucl. Phys. A **176** (1971) 65.
- [18] L. Coraggio, A. Covello, A. Gargano, N. Itaco, and T. T. S. Kuo: Ann. Phys. **327** (2012) 2125.
- [19] L. Coraggio, A. Covello, A. Gargano, N. Itaco, and T. T. S. Kuo: Prog. Part. Nucl. Phys. **62** (2009) 135.
- [20] T. Engeland: the Oslo shell-model code 1991-2006, unpublished.
- [21] N. Ayoub and H. A. Mavromatis: Nucl. Phys. A **323** (1979) 125.
- [22] H. M. Hoffmann, Y. Starkand, and M. W. Kirson: Nucl. Phys. A **266** (1976) 138.
- [23] K. Suzuki and S. Y. Lee: Prog. Theor. Phys. **64** (1980) 2091.
- [24] J. Shurpin, T. T. S. Kuo, and D. Strottman: Nucl. Phys. A **408** (1983) 310.
- [25] Data extracted using the NNDC On-line Data Service from the ENSDF database, file revised as of August 29, 2014.
- [26] W. Urban *et al.*: Eur. Phys. J. A **5** (1999) 239.